

Part II: Lévy walks as adaptive strategies

5

Helical Lévy walks in microzooplankton

5.1 Abstract

The searching trajectories of different animals can be described with a broad class of flight length (ℓ_j) distributions with $P(\ell_j) = \ell_j^{-\mu}$. Theoretical studies have shown that changes in these distributions (i.e., different μ values) are key to optimizing the long-term encounter statistics under certain searcher-resource scenarios. In particular, they predict the advantage of Lévy searching ($\mu \approx 2$) over Brownian motion ($\mu \geq 3$) for low-prey-density scenarios. Here, we present experimental evidence of predicted optimal changes in the flight-time distribution of a predator's walk in response to gradual density changes of its moving prey. Flight times of the dinoflagellate *Oxyrrhis marina* switched from an exponential to an inverse square power-law distribution when the prey (*Rhodomonas* sp.) decreased in abundance. Concomitantly, amplitude and frequency of the short-term helical path increased. The specific biological mechanisms involved in these searching behavioral changes are discussed. We suggest that, in a three-dimensional environment, a stronger helical component combined with a Lévy walk searching strategy enhances predator's encounter rates. Our results support the idea of universality of the statistical laws in optimal searching processes despite variations in the biological details of the organisms.

5.2 Introduction

Random walks based on Lévy flight distributions $P(\ell_j) = \ell_j^{-\mu}$ in concrete “Lévy walks” with $\mu \approx 2$, are the optimal searching strategy for scarce fixed targets which are randomly located (Viswanathan et al., 1999). A Lévy walk could be more efficient than the usual Gaussian (i.e., Brownian) motion as suggested by early works on microzooplankton (Levandowsky et al., 1988a,b; Klafter et al., 1989), although Brownian motion is generally assumed in reaction-diffusion predator-prey models. Recently, ecological examples of Lévy walks have been provided for a wide range of animal species (Heinrich, 1979; Klafter et al., 1989; Levandowsky et al., 1997; Cole, 1995; Focardi et al., 1996; Viswanathan et al., 1996; Atkinson et al., 2002). However, the theoretical study of more complex scenarios has shown that the advantage of Lévy searching over other types of motion is restricted to a set of prey densities, and mobility and size of the predator relative to the prey (Bartumeus et al., 2002; Viswanathan et al., 2002). Therefore, natural selection should favour flexible behaviors, combining different searching strategies (i.e., searching statistics) under different conditions. Here, we present experimental evidence that changes occur in both the short- and long-term searching statistics of a predator (*Oxyrrhis marina*), coinciding with density changes of its moving prey (*Rhodomonas* sp.). The specific biological mechanisms involved are also identified.

The marine heterotrophic dinoflagellate *Oxyrrhis marina* has two flagella, one transversal and one longitudinal, providing three types of movement: rotation, translation, and sudden directional changes (Levandowsky & Kaneta, 1987; Cosson et al., 1988). The flagellar apparatus of *O. marina* has been well studied at both the cellular (Cosson et al., 1988) and the ultrastructural level (Cachon et al., 1988). Continuous flagellar movements are responsible for simultaneous rotation and translation of organisms, giving rise to a helical path during movement. Normal helical motion is interrupted by sudden (60-100 ms) changes in direction in response to direct, local mechanical stimuli, the so-called “avoidance reaction”. However, this term does not embrace the wide variety of conditions under which this behavior is observed. Thus, the term **reorientation leaps** is preferred. Reorientation leaps in *O. marina* are generated by transient arrests of the longitudinal flagellum beat. These are accompanied by a switch from a backward to forward orientation (see figure 5 in Cosson et al. (1988)). Videotape observations of *O. marina* movements show that the helical path is usually straight with occasional smooth, albeit significant, changes in trajectory. These changes are due to momentary changes in the amplitude and frequency of the gyres in the helical path. Despite this feature, the

most efficient changes in trajectory are caused by the reorientation leaps. These specific and discrete reactions govern the long-term searching walk in *O. marina*.

To test the hypothesis that changes in the long-term searching behavior of *O. marina* occur as a response to resource availability, two independent experiments were performed by using culture inocula of *O. marina* at two different times of the year.

5.3 Methods

5.3.1 Experimental organisms and design

In both experiments, the dinoflagellate was grown in a 1-liter container under controlled temperature and light conditions using the smaller autotrophic flagellate *Rhodomonas* sp. as food source. Live samples were withdrawn at 24- or 48-h intervals and immediately videotaped for 2 weeks in experiment A, and for 1 week in experiment B. The two experiments were carried out several months apart and are considered replicate experiments. The movement of *O. marina* in a Palmer cell was videotaped by using a charge-coupled device camera attached to a stereomicroscope immediately after withdrawal from incubation containers. Also, samples were fixed with Lugol's solution for cell enumeration. Prey and predators ranged from 10^1 to 10^5 individuals per ml; predators increasing and prey decreasing through time in the two experiments. Random digital movies of 150 frames (12 frames per s in experiment A, and 8 frames per s in experiment B) were taken from the complete videofilm. The cell 2D positions Fig. 5.1 were analysed using the NIH IMAGE ANALYSIS software (National Institutes of Health, USA; <http://rsb.info.nih.gov/nih-image>). Trajectories, swimming velocities, and successive turning angles were determined.

5.3.2 Data analysis

The experimental data set comprised individual trajectory series for *O. marina* with a sampling length ranging from 10 to 180 walk steps, with usual values of ≈ 50 . Data in each of the experiments were grouped into three prey-density ranges, covering the three main resource scenarios, i.e., conditions typical of blooms ($1 \times 10^4 - 1 \times 10^5$ cells per ml), productive areas ($1 - 2 \times 10^3$ cells per ml), and open ocean ($1 \times 10^1 - 5 \times 10^2$ cells per ml). Included in the analyses were 192 and 372 individual positions and turning angle series for experiments A and B, respectively. Velocity estimates of *O. marina* were computed for each individual series as the Euclidean distance

between successive 2D positions. Mean velocities were computed for data series in each of the three prey-density ranges. In Fig. 5.1 the velocities and the trajectories of cells are shown.

x velocity fluctuation series were obtained by computing changes in x coordinate positions. A power spectrum analysis (Chatfield, 1984) was performed on each series. Spectra were averaged for all time series in each resource scenario and binned at 0.1 frequency intervals (see Fig. 5.2). We also computed, for each resource scenario, (i) the distribution of turning angles, measured as changes in direction at fixed time steps (≈ 0.1 s) and scaled from 0° to 180° (see Fig. 5.3) and, (ii) the distribution of flight-time intervals, the periods of time between changes in direction (Mandelbrot, 1982; Shlesinger et al., 1993, 1995). The distribution of flight times in each of the three resource scenarios (see Fig. 5.4) was taken as indicative of the average individual behavior. The individual and averaged spectra of velocity fluctuations were similar, giving support to this assumption.

5.4 Results

5.4.1 Velocity fluctuations

Mean velocities (computed as the Euclidean distances between two successive 2D positions) were $\approx 200 \mu\text{m} \cdot \text{s}^{-1}$. Standard deviations ranged from 93.18 to $128.58 \mu\text{m} \cdot \text{s}^{-1}$. No clear pattern of change of mean velocity was identified with decreases in resource availability. Therefore, swimming patterns were not related to changes in mean velocity in experiments (see Fig. 5.1).

The spectral analysis based on continuous x velocity fluctuations showed both helical path and reorientation leaps of *O. marina*. A high-frequency regime (HFR) and a low-frequency regime (LFR) were distinguishable in each spectrum (Fig. 5.2). HFR reflects the short-term changes, which include the helical path, while LFR reflects the long-term searching behavior and, thus, the reorientation leap statistics. As resources became scarce, a gradual and significant increase of a periodical signal was observed at ≈ 2 Hz (HFR). This periodical signal increased both in frequency and amplitude (i.e., mean $S(f)$ value and mean maximum $S(f)$ value ranging from 1 to 3 Hz, Table 5.1). The LFR of the spectra seemed to indicate a “1/f noise” ($S(f) \approx f^\beta, \beta \approx -1$) scaling persistence (Chatfield, 1984; Voss, 1989; Middleton et al., 1995), which decreased (lower LFR slopes) with decreasing resources. However, the influence of the periodical signal and the shortness of the series makes the interpretation

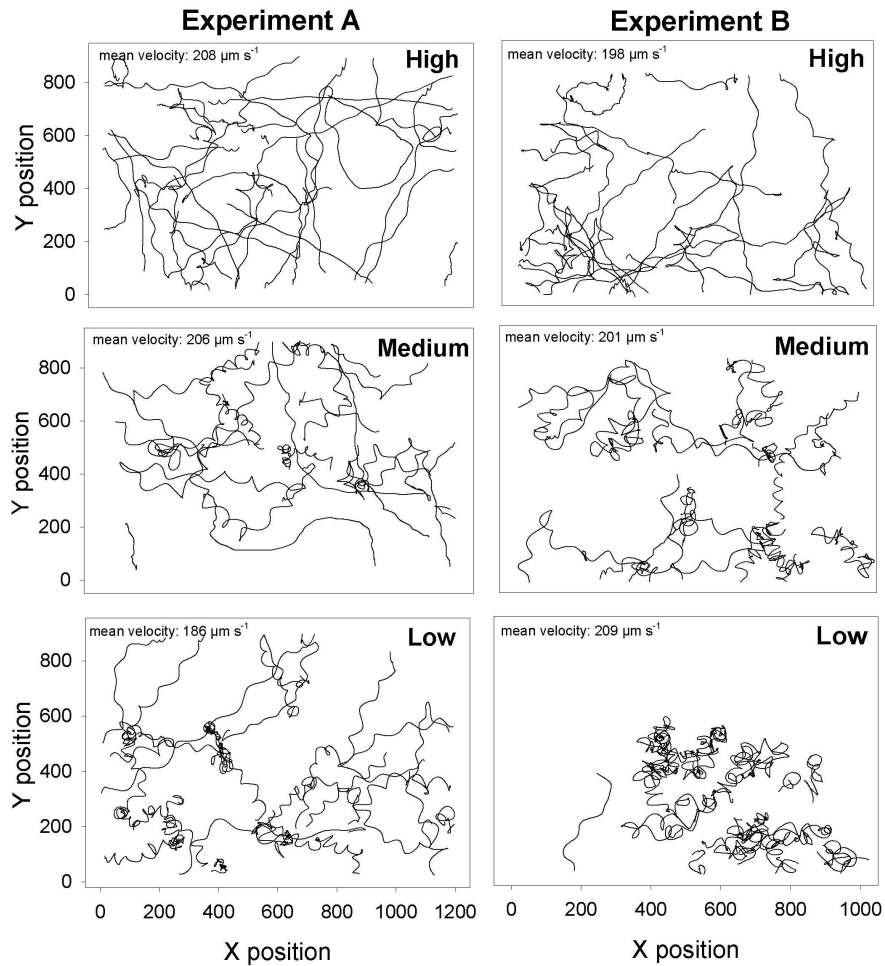


Figure 5.1: Representative 2D cell trajectories of *O. marina* in experiments A and B with various densities of *Rhodomonas* sp. prey: high ($1 \times 10^4 - 1 \times 10^5$ cells per ml), medium ($1 - 2 \times 10^3$ cells per ml), and low ($1 \times 10^1 - 5 \times 10^2$ cells per ml). The sampling effort has been fixed (i.e., the same number of walk steps in each resource scenario) to clarify the general searching pattern. An increase in the helical path as resources decrease is observed. At the scale of observation, Lévy walks visually result in a combination of short walk clusters with long travels between them, while Brownian walks look more like straight paths overcrossed. Thus, Brownian walkers cover the space more homogeneously than Lévy walkers do.

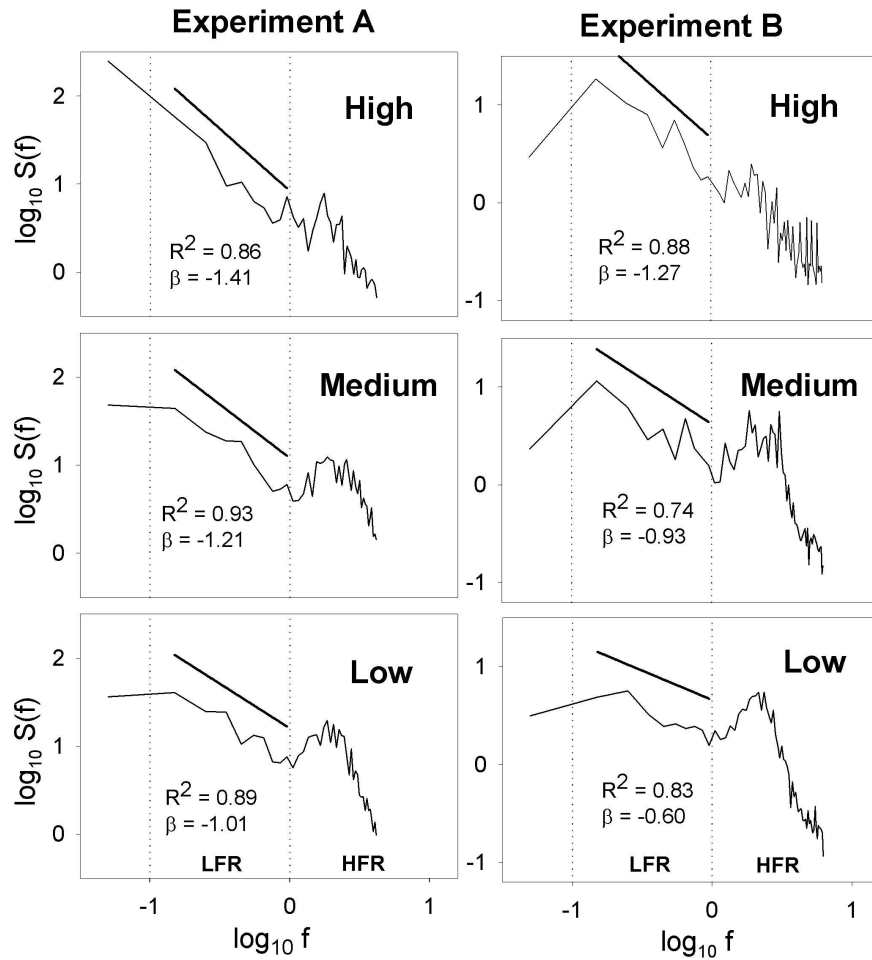


Figure 5.2: Log-log plots of the sum of power spectra [$S(f)$] against frequency (f), in hertz, in both experiments and each resource scenario. Vertical, dotted lines distinguish two frequency regimes: a HFR ($\log f > 0$) and a LFR ($\log f < 0$). A marked periodical signal at HFR (≈ 2 Hz) was observed with decreasing resources. At the LFR we defined the scaling exponent β by $S(f) \approx f^{-\beta}$; the least-square fittings are indicated by straight lines transposed upward for clarity, although the narrow range of the LFR makes the scaling questionable (see Fig. 5.4).

Table 5.1: Montecarlo randomization tests (n=1000) for mean $S(f)$ value and mean maximum $S(f)$ frequency (MMF) changes in the HFR periodical signal ranging from 1 to 3 Hz at different resource concentration scenarios.

Resource comparison	Experiment A		Experiment B	
	Mean $S(f)$	P	Mean $S(f)$	P
High vs. low	2.68 vs. 11.48	0.000	1.59 vs. 3.55	0.000
High vs. medium	2.68 vs. 8.15	0.000	1.59 vs. 3.19	0.000
Medium vs. low	8.15 vs. 11.48	0.007	3.19 vs. 3.55	0.341

Resource comparison	Experiment A		Experiment B	
	MMF	P	MMF	P
High vs. low	1.69 vs. 1.96	0.004	1.87 vs. 1.91	0.562
High vs. medium	1.69 vs. 1.99	0.004	1.87 vs. 1.99	0.185
Medium vs. low	1.99 vs. 1.96	0.740	1.99 vs. 1.91	0.248

of the LFR scaling questionable. Indeed, any nonscaling spectra could be approximated to a scaling spectrum at sufficiently narrow frequency ranges. Results were the same for y velocity-transformed series spectra, suggesting isometric conditions occurred during the experiment. Moreover, spectra of individual time series showed the same trends and similar periodical signal variances as the averaged series, indicating that the amalgamated population series that were analyzed, reflected individual behaviors.

5.4.2 Turning angles

The frequency distributions of turning angles as resources decreased (Fig. 5.3) showed a relative increase in intermediate-angle classes as compared with in low angle classes, particularly when resources changed from high to medium concentrations. In contrast, the distribution tails (large angles) were mostly uniform for the three resource scenarios. The angle class dividing the two histogram regions of contrasting response was the same for the three conditions (Fig. 5.3). The helical path involved mainly small turning angles: the larger the angle, the lower was its frequency, whereas reorientation leaps due to flagellar strokes usually caused strong cell reorientations (large turning angles). Therefore, based on data (Fig. 5.3), we chose 100° as the cut-off angle between helical paths and reorientation leaps. The latter govern the long-term searching walk and, thus, can be

considered as the effective turning angles. If effective directions were taken entirely at random, one would expect the mean angular deviation to be 90° . Deviations caused by active flagellar reorientation of cells have also been observed in other microorganisms, such as *Escherichia coli*, with an average (effective) turning angle of 103° (Berg, 1983b).

To improve the analysis of the long-scale component (i.e., for studying the macroscopic diffusion patterns), it might be desirable to subtract the helical path signal. Crenshaw and coauthors (Crenshaw et al., 2000) have appropriately characterized 3D helical tracks by means of the finite-helix-fit technique. However, even with a good description of the helical path, it is not straightforward to subtract the helicoid from the original trajectories of a number of individuals without significantly compromising the reliability of the long-term walk statistics. In the future, more accurate approaches for separating the two scale components may improve the characterization and understanding of the long-term searching behavior of microzooplankton. Nevertheless, our method (i.e., looking at the distribution of the turning angles), despite its crudeness, is sufficient to preserve the long-term signature of the walk.

5.4.3 Flight-time intervals

A statistical quantity characterizing long-term random walk patterns is flight-time interval, i.e., the period between two changes in direction (Mandelbrot, 1982; Shlesinger et al., 1993, 1995). Because changes in direction were mainly due to effective turning angles ($> 100^\circ$), the flight-time distributions were obtained by computing the time spent between them. As resources decreased from high to medium concentrations, we observed a change in flight-time distributions from exponential to power law in the searching behavior of *O. marina* (Pueyo, 2003). However, no substantial change occurred in flight-time distributions between medium and low concentrations (Fig. 5.4). A single value for the power-law exponents of $\mu \approx 2$ was found in the two experiments. When we randomly shuffled the data that gave rise to the power laws, the long-range correlations vanished and we recovered exponential laws as expected. Moreover, crude estimations of flight times between observable reorientation leaps on the standard *O. marina* movement videotapes gave the same qualitative results and exponents for the powerlaws ($\mu \approx 2$), showing a good relationship between real reorientation leaps and our effective turning criteria (turning angles $> 100^\circ$).

The exponential distributions of flight times in high resource scenarios gave rise to autoregressive random walks of order 1 (Chatfield, 1984).

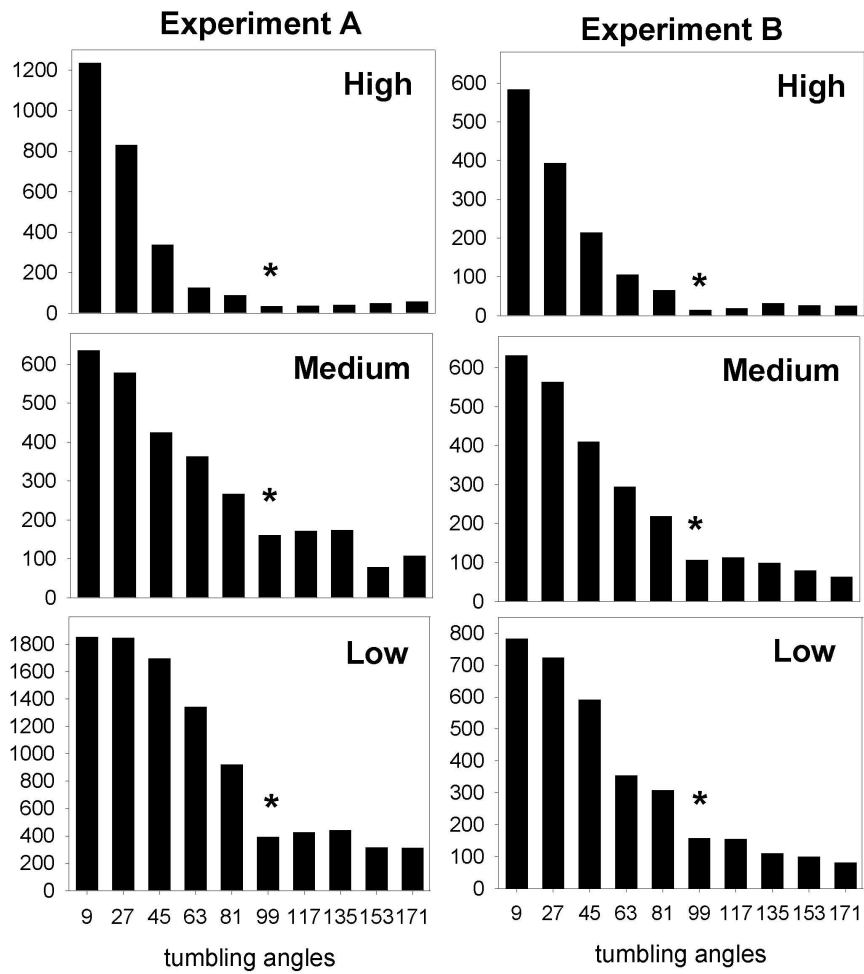


Figure 5.3: Turning-angle histograms scaled from 0 to 180°. Ordinate is number of observations. Asterisks in histograms mark the main discontinuity observed (class 90 – 108°).

In these so-called Markov chains, the probability of changing direction is independent of the time walked. Positions depend on previous walk steps, but long-range correlations are not expected. Exponential laws, through the Central Limit Theorem, give rise to asymptotically Gaussian statistics (Brownian motion), and, therefore, macroscopic normal diffusions are expected, the spreading variance of organisms being proportional to time (Weeks & Swinney, 1998).

When resources are scarce, power-law distributions of flight times with scaling exponents $\mu \approx 2$ give rise to the so-called Lévy walks. Also, the points where effective turnings occur correspond to the points visited during a Lévy flight (Shlesinger et al., 1995). These distributions involve long-range correlations, scale-invariance, and superdiffusion phenomena (Weeks & Swinney, 1998). The probability of long travels while swimming is higher than for random walks with exponential distribution of flight times. The slight deviations from pure power laws, observed mostly when resources were scarce (i.e., low-resource scenario) could be caused by swimming interference between individuals (videotape observations). In our experiments, low prey numbers coincided with high predator concentrations (10^4 cells per ml). Interference by predators could modify the intermediate flight length regime by increasing reorientation leaps while swimming (da Luz et al., 2001). In these cases, these leaps maybe truly “avoidance reactions” between predators.

5.5 Discussion

The searching behavior of individuals is, at least in part, genetically encoded. Therefore, we should expect natural selection to operate on genetic variability in perceptual and motor traits underlying both behavioral decision-making and response times in the location of resources (Bell, 1991). Thus, the ability of an organism to optimize its encounter rate in a complex and variable environment should be honed and sharpened through evolution (Catalan, 1999). In *O. marina*, searching behavior is adjusted in relation to resource concentration by two mechanisms controlled by flagellar movement: (i) at short scales, by amplitude and frequency changes in the helical path, involving continuous regulation of energy investment in the beating of transverse and longitudinal flagella; and (ii) at long scales, by changes in the statistics of reorientation leaps controlled by discrete strokes of the longitudinal flagellum.

Our observations suggest that the control of flagellar movement by *O. marina* admits two extreme searching behaviors in natural environments

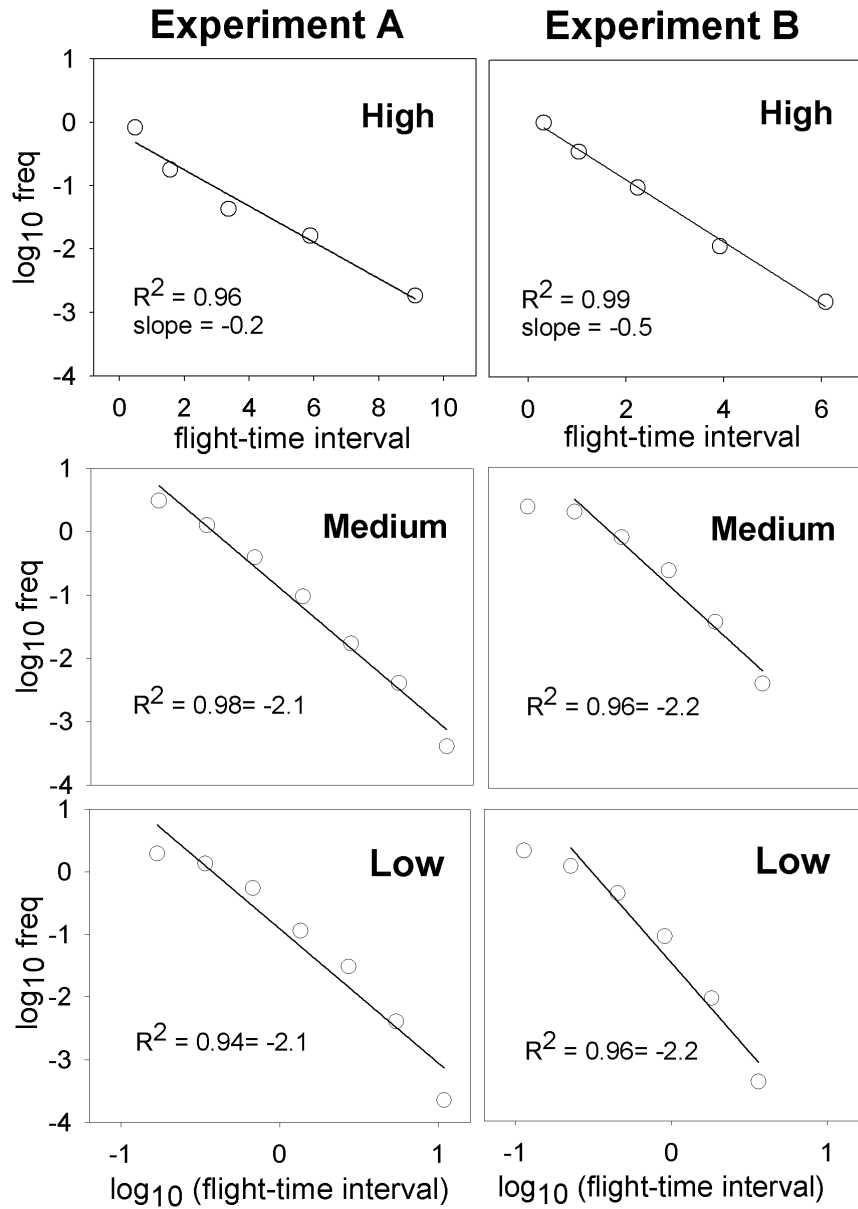


Figure 5.4: Log-linear (high-resource scenario) and log-log (medium- and low-resource scenarios) plots showing the frequency distribution of flight times at each resource scenario in both experiments. We used bin widths of 2^k for the bin k and geometric midpoints of bins to plot the results. Straight lines show the least-squares fitted regressions. The first point in experiment B at medium- and low-resource scenarios was spuriously underestimated due to finite scale effects and, thus, was not fitted.

with a multiplicity of intermediate behaviors between them. When resources are readily available, *O. marina* invests more energy in movement using the longitudinal flagellum (continuous movement combined with strokes) than in movement using the transverse flagellum. Thus, the helical path follows a near-linear axis, due to low amplitude and frequency of gyres. On the other hand, in medium- and low-resource scenarios, the most common in nature, *O. marina* invests more energy in movement using the transverse flagellum, which results in 3D large helicoid trajectories, and in changing the statistics of the longitudinal flagellum strokes, determining the scale-invariant Lévy random searches with scaling exponent $\mu \approx 2$.

Fig. 5.1 shows that Lévy walks do not consist simply in adding long walks to a Brownian motion. The two types of motion differ in the whole flight-time probability distribution (i.e., short and long flight times). Lévy walks not only involve a fat tailed flight-time probability distribution (i.e., long travels), but also a “scaling” of all flight times (i.e., no characteristic size of flight-time intervals exists). Once an observational scale is fixed, a power-law distribution of flight times (i.e., a Lévy walk) turns out to be a combination of “walk clusters” with long travels between them, giving rise to an heterogeneous multiscale-like sampling effort pattern. On the other hand, an exponential distribution of flight times (Brownian walks) gives rise to a mostly spatially homogeneous sampling effort pattern (Fig. 5.1). In comparing Brownian and Lévy motions with the same sampling effort, differences in the general searching pattern will appear at any scale of observation, because these differences are caused by the scaling vs. nonscaling global property of the two flight-time distributions. However, the specific consequences of the increase in the frequency of long flight times (i.e., short vs. fat tailed distributions) will not be observed until sufficiently large spatiotemporal scales of observation are reached. Thus, at certain scales of observation, Lévy walks may not be translated into an observational macroscopic super-diffusion of cell populations (i.e., the spreading variance of organisms being “more than” proportional to time) or into an observable decrease of individual re-sampling of the self-backtrails. Moreover, in *O. marina*, both effects caused by the fat tail of the Lévy walk flight-time distribution are even more difficult to observe because long travels have a strong helical component. Thus, each long time travel becomes shorter in terms of path length (i.e., linear distance travelled) than in the Brownian case (high-resource levels), where the straighter paths determine larger path lengths.

In a 3D world, and given enough time, the probability for a Brownian random walker to revisit the same point is only about 0.35, while in one and two dimensions this probability converges to 1 (Feller, 1968). There-

fore, in a 3D fluid world, changes from a Brownian to a Lévy walk may not be caused by the need for the walker to avoid re-sampling his self-backtrails. Rather, it may be caused by the possibility of sampling a given region combining different sizes of walk clusters and long travels at different scales (i.e., a multiscale, multifractal-like pattern (Jaffard, 1999; Nakao, 2000)). Indeed, theoretical models have shown that even in 2D nondestructive foraging (i.e., where resampling could not be so bad to improve encounter rates) Lévy walks are better than Brownian when resources are scarce (Viswanathan et al., 1999, 2002). Conversely, they show Brownian motion not as a null model, which should be improved because of high re-sampling rates, but as another searching strategy which is optimal under certain conditions (i.e., high-resource levels (Bartumeus et al., 2002)). Our results confirm the theoretical expectation of a switching behavior between Brownian and Lévy strategies as an optimal solution in different resource scenarios.

Then, the question turns out to be, what is the advantage to *O. marina* of performing “helical Lévy walks” instead of pure Lévy walks? Why did *O. marina* increase its helical movement component as resources decreased? Several hypothesis can be suggested, including both statistical or energetical considerations, in order to explain the observed change of behavior. A walker in a 3D environment, in comparison with a 2D one, not only should have less probability of resampling its own self-backtrails, but it also should have more probability of “missing” near targets. Therefore, we suggest that larger helical paths should lead to more efficient 3D micro-scale explorations. Given the possibility that dinoflagellates use their chemosensory abilities (Hauser et al., 1975) to find their prey, the radius and the pitch of the helicoid (Ricci, 1992) should be larger than the nearby space covered by organisms’ sensorial structures to have an efficient search. Larger helical paths may also increase the long-term Lévy walk statistical efficiency of encounters by avoiding midterm curvilinear biases of long travels (Levandowsky & Kaneta, 1987; Kamykowski et al., 1992). Moreover, while following large helicoids, *O. marina* invests more energy in movement using the transverse flagellum than the longitudinal one. Experimental reactivation of isolated and permeabilized flagella of *O. marina* suggests that energetical requirements for both flagella are similar (Cosson et al., 1988). Therefore, if some energetic advantage is involved in performing larger helical paths, it should be related not to the differential use of flagella but to other factors.

A good 3D search should involve both short- and long-term efficient searching strategies. Optimal long-term searching strategies are independent of the dimension of the foraging space (Bartumeus et al., 2002;

Viswanathan et al., 2001a) but this independence may not hold for the short-term component of a searching process which may change with the number of dimensions used in the exploration. The possibility that, in a 3D environment, the incorporation of large helical paths (i.e., as a short-scale searching strategy) improves the statistics of encounters by decreasing the probability of “missing” near targets and/or by avoiding midterm curvilinear biases, or whether it reduces some energetic costs, remains an open question that needs further consideration.

In conclusion, we suggest that the chance of finding food in 3D environments, depends not only on the *path lengths* (i.e., linear distances traveled) but also on the *whole shape* of the walk. Long path lengths mainly explain the avoidance of resampling back-trails but, as we have argued, is not necessarily the key aspect for optimizing encounters in a 3D exploration. Efficient sampling in a low-Reynolds number 3D environment without cues may be based not on rapidly avoiding regions with scarce resources, but on exploring the whole environment at the largest range of possible scales while maintaining an efficient local exploration (whether energetic or statistical) of the 3D environment. Based on these sampling requirements, we suggest that helical Lévy walks optimize random searching (i.e., number of encounters with prey) in 3D environments with low prey densities. Helical Lévy walks may be as widely spread among dinoflagellates (Kamykowski et al., 1992) and other microzooplankters (Ricci, 1992), as pure fractal (Coughlin et al., 1992) and multifractal (Schmitt & Seuront, 2001) random walks are among macrozooplankters. However, a variety of specific motion mechanisms could be involved in this type of random searching motion.

Further, our results are consistent with the hypothesis that the exponent $\mu_{opt} = 2$ may be universal, i.e., independent of the dimension of the foraging space (Viswanathan et al., 2001b; Bartumeus et al., 2002) and robust with respect to short-scale effects, including effects on the organisms' behavior and physiology (Peters, 1994; Yamazaki & Kamykowski, 2000; da Luz et al., 2001). The example given here demonstrates the usefulness of random search theory for providing a more realistic view of ecological interactions. We hope our case-study will encourage ecologists to reexamine the hitherto, traditionally applied “mean field” assumption in ecological theory.

Acknowledgements

F.P. and C.M. designed and performed the experiments; F.P. prepared the procedure for image analyses. The methods and criteria for data analyses were established by S.P. and F.B. (with a larger contribution from S.P.) and applied by F.B.; the text was written by F.B. and J.C. with input from all coauthors. We thank M. Castaño, A. Lorente, and J. Piera for help at different stages of this work and for discussions, and two anonymous reviewers for comments on the manuscript. D. Balayla revised the English typescript. F.B. was the recipient of a Comissió Interdepartamental de Recerca i Innovació Tecnològica fellowship (1997FI 00296 UB APMARN). F.P. received a European Union post-doctoral grant (ERBFMBICT950195) and acknowledges the support of the European Union project Nutrient Dynamics Mediated through Turbulence and Plankton Interactions (EVK3-CT-2000-00022). This article is European Land Ocean Interaction Studies Contribution 402/40.

6

Animal search strategies: a random walk analysis

6.1 Abstract

Recent advances in spatial ecology have improved our understanding of the role of large-scale animal movements. However, an unsolved problem concerns the inherent stochasticity involved in many animal search displacements and its possible adaptive value. When animals have no information about where targets (i.e., resource patches, mates, etc.) are located, different random search strategies may provide different chances to find them. Assuming random walk models as a necessary tool to understand how animals face such environmental uncertainty, we analyze the statistical differences between two random walk models commonly used to fit animal movement data, the Lévy walks and the correlated random walks, and we quantify their efficiencies (i.e., the number of targets found in relation to total displacement) within a random search context. Correlated random walk properties (i.e., scale-finite correlations) may be interpreted as the by-product of locally scanning mechanisms. Lévy walks, instead, have fundamental properties (i.e., super-diffusivity and scale invariance) that allow a higher efficiency in random search scenarios. Specific biological mechanisms related to how animals punctuate their movement with sudden re-orientations in a random search would be sufficient to sustain Lévy walk properties. Furthermore, we investigate a new model (the Lévy-modulated correlated random walk) that combines the properties of correlated and Lévy walks. This model shows that Lévy walk properties are robust to any

behavioral mechanism providing short-range correlations in the walk. We propose that some animals may have evolved the ability of performing Lévy walks as adaptive strategies in order to face search uncertainties.

6.2 Introduction

Standard methods in spatial ecology assumed Brownian motion and Fickian diffusion as two basic properties of animal movement at the long-term limit (i.e., large spatial scales and long temporal scales). Thus, it is assumed that animal movements can be modelled (at the long-term limit) as *uncorrelated random walks* (Okubo, 1980; Berg, 1983a). The problem of *uncorrelated random walks* is that they do not account for directional persistence in the movement (i.e., the tendency by animals to continue moving in the same direction). Such limitation was overcome with two different types of random walks, correlated random walks (CRWs) and Lévy walks (LWs).

CRWs appeared in ecology from the analysis of short and middle-scaled animal movement data. Experiments with ants, beetles, and butterflies were performed in less than 25 square meter arenas, or otherwise, in their natural environments, and usually last less than an hour (e.g. (Bovet & Benhamou, 1988; Turchin, 1991; Crist et al., 1992)). From these studies, ecologists promptly became aware of the necessity of adding directional persistence into pure random walks to reproduce realistic animal movements (Kareiva & Shigesada, 1983; Bovet & Benhamou, 1988). More recently, the mathematical properties of CRWs were used to explore the link between individual animal movements and population level spatial patterns (Turchin, 1991, 1998). Further studies have considered the relative straightness of the CRW i.e., degree of directionality (Haefner & Crist, 1994), or sinuosity (Bovet & Benhamou, 1991; Bovet & Bovet, 1993; Benhamou, 2004), as relevant properties characterizing animal movement.

The analysis of animal movement at larger spatial scales or at longer temporal scales has given rise to a new category of random walk models known as Lévy walks (Levandowsky et al., 1988a; Viswanathan et al., 1996). Animal paths involving large spatial or temporal scales (i.e., large-scale animal movement), turn out to be a combination of “walk clusters” with long travels between them. The heterogeneous multiscale-like sampling pattern generated by such paths are closely related to fractal geometries (Mandelbrot, 1977) and better modeled by random walks with Lévy statistics. LWs have their origin in the field of statistical mechanics and find wide application in physics (Shlesinger et al., 1995; Klafter et al., 1996; Weeks & Swinney, 1998) and natural sciences such as geology and

biology (Metzler & Klafter, 2004). Although they have recently gained attention in optimal foraging theory (Viswanathan et al., 1996, 1999), they appeared in an ecological context around the same decade as CRWs. The first mention of Lévy walks as animal search strategies can be found in Shlesinger & Klafter (1986) (see page 283). After that, Lévy walks were formally considered by plankton ecologists (Levandowsky et al., 1988a,b; Klafter et al., 1989).

CRW and LW models have been adjusted successfully to a wide range of empirical data (**CRWs**: Kareiva & Shigesada (1983); Bovet & Benhamou (1988); Turchin (1991); Crist et al. (1992); Johnson et al. (1992); Bergman et al. (2000); **LWs**: Viswanathan et al. (1996); Levandowsky et al. (1997); Atkinson et al. (2002); Bartumeus et al. (2003); Ramos-Fernández et al. (2004)). Recent works have introduced the idea of hierarchical scale-adjustments on animal displacements (Fritz et al., 2003), and have fitted field data of specific species (Marell et al., 2002; Austin et al., 2004) by using both models. All these studies have shown that CRWs and LWs can be used as fitting procedures to analyze animal movement. Nevertheless, there is a lack of an explicative framework for such an approach, which severely limits the biological interpretation of the obtained results. A better understanding of random searching processes may help to develop random walk models with sound *explicative power* sensu Ginzberg & Jensen (2004). This knowledge could clarify how animals face environmental uncertainty and reduced perceptual capabilities in large-scale displacements (Lima & Zollner, 1996). Further, a solid relationship between animal behavior and the statistical properties of movement could be established, thus uncovering useful links between the behavioral (Bell, 1991) and the pattern-based approaches common in spatial ecology (Okubo, 1980; Tilman & Kareiva, 1997).

Although some theoretical studies have already shown the potential role of CRWs and LWs in the understanding of animal random search strategies (Zollner & Lima, 1999b; Viswanathan et al., 1999), two fundamental questions about CRW and LW models still need to be addressed. First, quantifying their efficiency as random search strategies based on their respective statistical and scaling properties. Second, developing adequate biological interpretations of such properties in a random search context. The present contribution is a first effort to clarify the above points. For doing so, we have structured our analysis as follows. First, we demonstrate quantitatively relevant differences in the statistical properties of CRWs and LWs. Then, we discuss how such properties explain the different efficiencies obtained when the models are used as random search strategies in the ecological context. Finally, we suggest how the present results may

lead to a better theoretical understanding of some fundamental aspects of large-scale animal displacements in real ecosystems. We would like to emphasize that our goal is not to provide recipes to analyze specific empirical data and determine which models would lead to a better fitting in a particular case. Instead, our purpose is to provide general criteria to evaluate *why* we should expect one of the models to fit better. Providing explicative power to random walk models is especially necessary if such models are going to be used as null models, as well as if deviations from such null models are going to be interpreted biologically.

6.3 Methods

Random walks constitute probabilistic discrete step models that involve strong simplifications of real animal movement behavior. In relation to more complex behavioralist models including many parameters, random walk models ultimately express behavioral minimalism (Lima & Zollner, 1996; Turchin, 1998). Their main basic assumption holds that real animal movements consist of a discrete series of displacement events (i.e., move lengths) separated by successive reorientation events (i.e., turning angles). Discretization of complex movement behaviors will determine (after a large enough number of successive moves) the statistical distribution of displacement lengths on the one hand, and the statistical distribution of changes of direction (i.e., turning angles) on the other hand. From successive random draws of such distributions, we can obtain different movement path realizations. All the paths obtained by this method have statistical equivalence.

6.3.1 The models

We have used three random walk models in our quantitative analysis. Correlated random walks (CRWs), Lévy walks (LWs), and a new model based on the previous ones which we have named Lévy-modulated correlated random walks (LMCRWs). Each model controls the directional persistence of the movement (i.e., the degree of correlation in the random walk) in a different way. Below we briefly discuss each model and the simulation procedures, leaving to the Appendix 6.6 all the technical details.

CRW models (see Appendix 6.6.1) combine a Gaussian (or other exponentially decaying) distribution of move lengths (i.e., displacement events) with a non-uniform angular distribution of turning angles (i.e., reorientation events). These models control directional persistence (i.e., the degree of correlation in the random walk) via the probability distribution of turn-

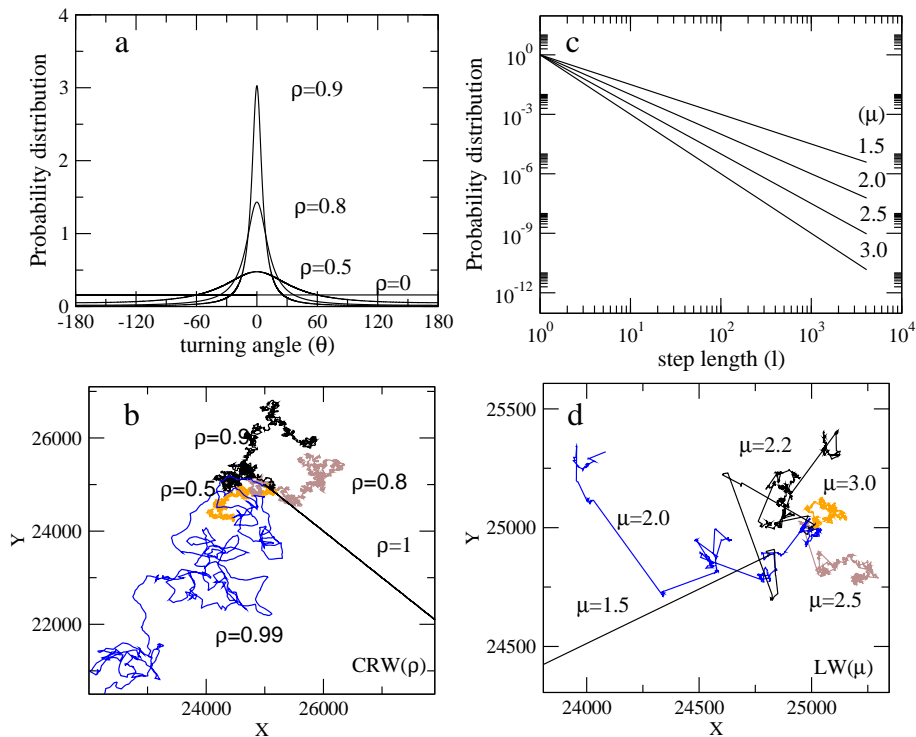


Figure 6.1: (a) Shape of the wrapped Cauchy distribution used in the correlated random walk, for different values of the shape parameter ρ . (b) Examples of correlated random walks, generated by wrapped Cauchy distributions with different shape parameters. (c) Power-law distributions used in the Lévy walk, for different values of the Lévy exponent μ . (d) Examples of Lévy walks, generated by power-law distributions with different Lévy exponents.

ing angles. In our study, we have used a wrapped Cauchy distribution (WCD; Batschelet 1981; Haefner & Crist 1994) for the turning angles. Directional persistence is controlled by changing the shape parameter of the WCD (ρ). For $\rho = 0$ we obtain a uniform distribution with no correlation between successive steps, thus Brownian motion emerges. For $\rho = 1$ we get a delta distribution at 0° (Fig. 6.1a), leading to straight-line searches (Fig. 6.1b).

LW models (see Appendix 6.6.2) involve a uniform distribution for the turning angles, but a power-law distribution for the move lengths (i.e., the so-called flights). The exponent of the power-law is named Lévy index ($1 < \mu \leq 3$, see Fig. 6.1c) and controls the range of correlations in the movement. LW models thus comprise a rich variety of paths ranging from

Brownian motion ($\mu \geq 3$) to straight-line paths ($\mu \rightarrow 1$) (Fig. 6.1d).

Finally, the LMCRW model (see Appendix 6.6.3) here introduced generates a random walk with (i) a WCD for the turning angles within a flight, (ii) a Gaussian distribution of move steps within a flight, (iii) a uniform distribution for the turning angles between flights, and (iv) a power-law distribution of flight lengths. As in the LW model, the directional persistence of LMCRW is also introduced through a power-law distribution of move lengths (i.e., flights) but we can also modulate or control the degree of directional persistence during flight lengths through a WCD of turning angles (i.e., by changing the value of ρ). This new model can reveal which type of directional persistence controls the optimization of random searches, whether the power-law distribution of move lengths or the WCD of turning angles.

6.3.2 The simulations

The statistical properties of random walk models should be evaluated at the long-term limit (i.e., large spatial scales and long temporal scales). When running simulations, this means that both the turning angle and the move length probability distributions should be thoroughly sampled (i.e., which is especially important with long-tailed probability distributions). The *long-term* statistical properties of random searches only emerge once included a minimum amount of time and space in the search. The spatiotemporal scales required for that are not fixed, but organism specific.

A first group of simulations studied the behavior of a relevant macroscopic property of random walks: the mean square displacement (msd), defined as the squared distance that an organism moves from its starting location to another point during a given time, averaged over many different random walkers. Msd is related to the CRW metric of net squared displacement but is not exactly the same (see Appendix 6.6.4 for more details). In these set of simulations we computed the msd for a set of random walkers moving in a two-dimensional arena at different times considering different parameter values for ρ and μ in CRWs and LWs respectively.

We devised a second group of simulations in order to determine the search efficiencies ($\lambda\eta$) of the three types of random walks (i.e CRW, LW and LMCRW models). The objects that are looked for are named targets. In general, a target may represent any important resource for a searcher (i.e., food, mates, breeding habitats, nesting sites, etc.). In our simulations targets are non-mobile, thus we prefer the term target sites (e.g., static resources, suitable habitats, etc.). We defined the search efficiency function η as the ratio of the number of target sites visited to the total distance

traversed by the searcher. Note that in LWs $\eta = \eta(\mu)$, in CRWs $\eta = \eta(\rho)$, and in the LMCRWs $\eta = \eta(\mu, \rho)$. Specifically, the simulations quantified the average search efficiency of a set of random walkers provided with a radial detection distance r_d , that looked for non-mobile circular items with radius r_t (i.e., target sites) in a two-dimensional space with periodic boundary conditions. Target sites were uniformly distributed in an otherwise homogeneous arena. The scaling of the search scenarios is based on a unique key parameter: the mean free path (λ), which is defined as the average distance between two target sites. The mean free path is inversely related to target sites density and searcher's detection radius and give us the idea of how far the searcher moves before "detecting" a target (see Appendix 6.6.5). We defined three different search scenarios with increasing values of λ representing a decreasing gradient of target site densities (we keep the same searcher's detection radius for the three search scenarios). To represent different search strategies, we run the simulations using different parameter values for each random walk model (i.e., LW and CRW). The product $\lambda\eta$ allows us to obtain a metric for the search efficiency that is independent of the target site density.

We considered two kinds of encounter dynamics in the efficiency simulations: destructive and non-destructive. In the case of non-destructive searches, the searcher can visit the same target site many times. This accounts for those cases in which target sites become only temporarily depleted or searchers become satiated and leave the area. In the case of destructive searches, the target site found by the searcher becomes undetectable in subsequent displacements, the target site "disappears." In this case, just to make averages always with the same target density, we generate a new target site at random in the searching space. Both types of encounter dynamics may represent real ecological situations and should demand different random search strategies in order to optimize the rate of encounters (Viswanathan et al., 1999). The non-destructive and destructive searching scenarios represent the limit cases of a continuum of possible target regeneration dynamics (Raposo et al., 2003). Moreover, the non-destructive case with uniformly distributed targets bears a similarity to a destructive case with patchy or fractal target-site distributions (Viswanathan et al., 1999). Thus, these simulations cover a wide range of natural searching scenarios.

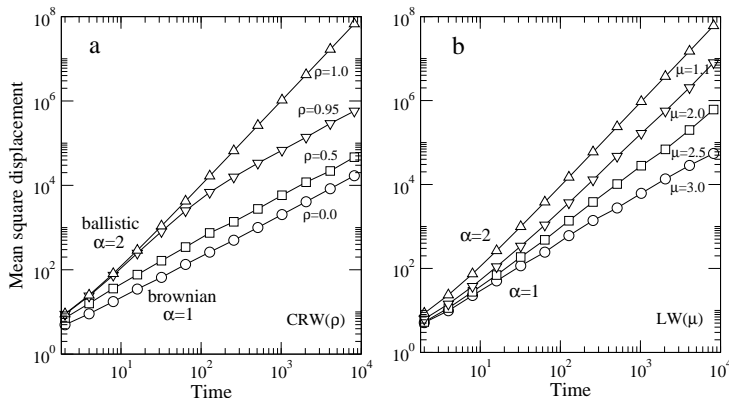


Figure 6.2: Mean square displacement (msd) in relation to time for (a) Correlated random walks and (b) Lévy walks. The scaling behavior indicates short ($\alpha = 1$) and long-range ($\alpha > 1$) correlations in the random walks. $\alpha = 2$ indicates ballistic (i.e., straight-line) motion. Msd was obtained averaging 500 individuals.

6.4 Results

6.4.1 On the macroscopical properties of CRWs and LWs

Random walk theory assumes that a particularly relevant macroscopic property of random walks involves the scaling in relation to time of the mean square displacement (msd) of the diffusing organisms: $\langle R(t)^2 \rangle \sim t^\alpha$, where α characterizes the behavior of diffusive processes. In normal (i.e., Fickian) diffusive processes the msd increases linearly with time ($\alpha = 1$). The most simple example of this, is when particles (or organisms) move independently and execute uncorrelated random walks i.e., pure Brownian motion. On the other hand, processes that lead to a nonlinear dependence of msd over time, known as anomalous diffusion, typically occur in complex or long-range correlated phenomena (Gefen et al., 1983). Anomalous diffusion arises due to long-range statistical dependence between steps in a random walk and can involve a sub-diffusive ($\alpha < 1$) or a super-diffusive ($\alpha > 1$) process. The fastest possible super-diffusion occurs when particles (or organisms) execute unbroken straight-line paths corresponding to ballistic motion or dispersal with $\alpha = 2$.

As stated above, CRW models control persistence (i.e., the degree of correlation in the random walk) via the probability distribution of turning angles. However, from the macroscopic point of view, CRWs represent simple Markovian processes that, by their very nature, cannot generate long-range correlations in the movement (Johnson et al., 1992). Thus, for

CRWs the msd can depart from the linear increase with time only over a particular range of temporal and spatial scales, but at the long-term limit the relation always becomes linear. Therefore, at the long-term limit CRWs models appear like uncorrelated random walks: they only can give rise to Brownian motion. Fig. 6.2a shows the behavior of the msd in a CRW as we vary the shape parameter ρ of the WCD (used to correlate the steps). For any value $\rho < 1$ (even for values close to 1, i.e., $\rho = 0.95$) the macroscopic behavior of movement converges rapidly ($t \approx 100$) to the Brownian motion domain. Only for the limit case of $\rho = 1$ do we obtain a ballistic motion. Thus, there is no a smooth way to go from Brownian to ballistic motion by changing the turning angle distribution parameter of CRWs (ρ). Instead, only two macroscopic motions emerge in the long term limit: pure Brownian ($\rho < 1$) or ballistic dispersal behavior ($\rho = 1$).

When persistence arises through a power-law distribution of move lengths instead of Markovian short-range angle correlations, a new property emerges because of long-range move length correlations. A gradual change in the Lévy exponent (i.e., μ) corresponds to a gradual change in the diffusivity (i.e., α) that does not vanish at the long-term limit. A gradual transition from normal diffusion ($\alpha = 1$ for $\mu \geq 3$) to ballistic motion ($\alpha \rightarrow 2$ for $\mu \rightarrow 1$) becomes possible for LWs (Fig. 6.2b). Therefore, different Lévy exponents of the power-law distribution of move lengths provide a whole variety of super-diffusive behaviors ($1 < \alpha < 2$ for $1 < \mu < 3$). Thus, changing the Lévy exponent implies a qualitative change in the macroscopic and long-term properties of the movement as a whole.

6.4.2 On the search efficiency of the random walk models

Fig. 6.3 shows the changes in the searching efficiency measured as $\lambda\eta$ of both a CRW ($\eta(\rho)$) and a LW ($\eta(\mu)$) when varying the parameters controlling the degree of persistence in the walk. We have considered three search scenarios ($\lambda = 100, 1000$ and 5000 , see Methods and Appendix 6.6.5) representing a decreasing gradient from high to low target densities, and two encounter dynamics, destructive and non-destructive.

In all cases, LWs are more efficient than CRWs. As density diminishes (i.e., λ increases), LWs become even more efficient (than CRWs) in both dynamical types of searches, but with different optimal Lévy exponents (μ_{opt}). In the destructive case $\mu_{\text{opt}} \rightarrow 1$ and in the non-destructive case $\mu_{\text{opt}} \approx 2$. These results agree with previous works on Lévy walk random searches (Viswanathan et al., 1996, 1999). Note the convergence of CRWs ($\rho = 0$) with LWs ($\mu = 3$) and CRW ($\rho = 1$) with LW ($\mu \rightarrow 1$). In the former, both models correspond essentially to Brownian motion, whereas in the lat-

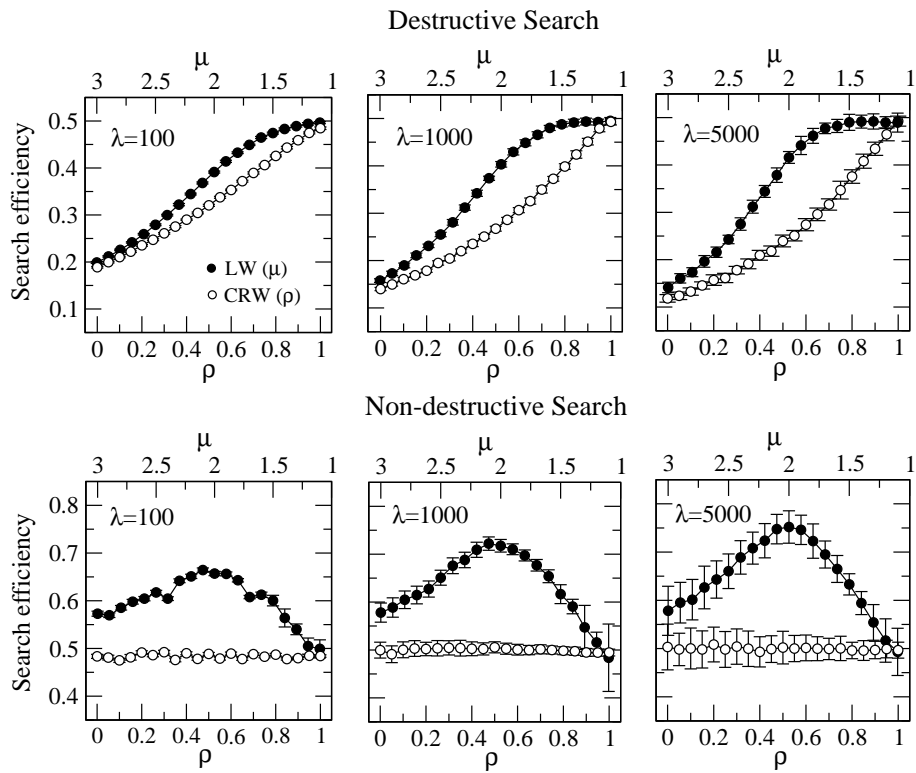


Figure 6.3: Comparison of the search efficiency (measured as $\lambda\eta$) of different animal search strategies. The panels assume three different target densities ($\lambda = 100, 1000$, and 5000 , respectively). The three top panels assume that the targets are destroyed once found, whereas the three bottom panels assume that the targets are not destroyed. Search efficiency is plotted as a function of the shape parameter ρ for correlated random walks (open circles) and as a function of the Lévy exponent μ for Lévy walks (closed circles).

ter they give rise to straight-line motion (i.e., ballistic dispersal behavior). The relevant differences appear precisely in the transition from Brownian to ballistic motion. Within the whole range of possible random walks from the Brownian (pure random walk) to the ballistic (straight-line walk), searchers performing LWs exhibit higher efficiency than searchers performing CRWs in the long-term encounter statistics (i.e., $\eta(\mu_{\text{opt}}) \geq \eta(\rho_{\text{opt}})$ in Fig. 6.3).

In destructive searches (Fig. 6.3), revisiting target sites penalizes the search efficiency because targets are consumed. Therefore, the larger the persistence in the movement the larger the search efficiency. Persistence increases with increasing ρ in CRWs and decreasing μ in LWs. However, changes in Lévy exponent not only modify short-term persistence of the walk but also involve concomitant changes in the macroscopic properties of the movement that the CRWs do not have. As μ decreases super-diffusivity of movement is enhanced (see Fig. 6.2). Super-diffusion increases the efficiency beyond short-ranged persistence, that is why LWs are more efficient than CRWs in destructive searches.

In non-destructive searches (Fig. 6.3), revisiting sites is not penalized because targets are not consumed. Therefore, persistence and super-diffusivity do not influence search efficiency significantly. Indeed, they are only useful to avoid empty areas created by destructive encounter dynamics. This fact explains why the efficiency of CRWs in the non-destructive case is ρ -independent. However, the higher values for the LWs efficiency (which furthermore remains dependent on μ) maybe due to another particular LW property not shared with CRWs, namely, scale invariance. Thus, our results clearly show that scale invariance plays a crucial role in optimizing encounter rates in the non-destructive cases.

Fig. 6.4 shows the searching efficiency measured as $\lambda\eta$ for the LMCRW model $\eta(\mu, \rho)$ and $\lambda = 5000$ in destructive and non-destructive searches. Changes in the ρ and the μ parameters account for different searching strategies with different searching efficiencies. For the destructive case ρ must be very close to 1 (i.e., move lengths must be straight lines) in order to get optimal searches. However, for the non-destructive case a certain degree of sinuosity during move lengths (i.e., $0.8 < \rho < 1$) does not diminish the searching efficiency considerably. In non-destructive searches, as the degree of persistence within flights diminishes, the overall efficiency of the search diminishes and the Lévy index giving rise to optimal searching strategies also decreases.

The LMCRW model results for non-destructive dynamics (Fig. 6.4), show that reorienting the movement at power-law time intervals have more influence in the search efficiency than small direction deviations

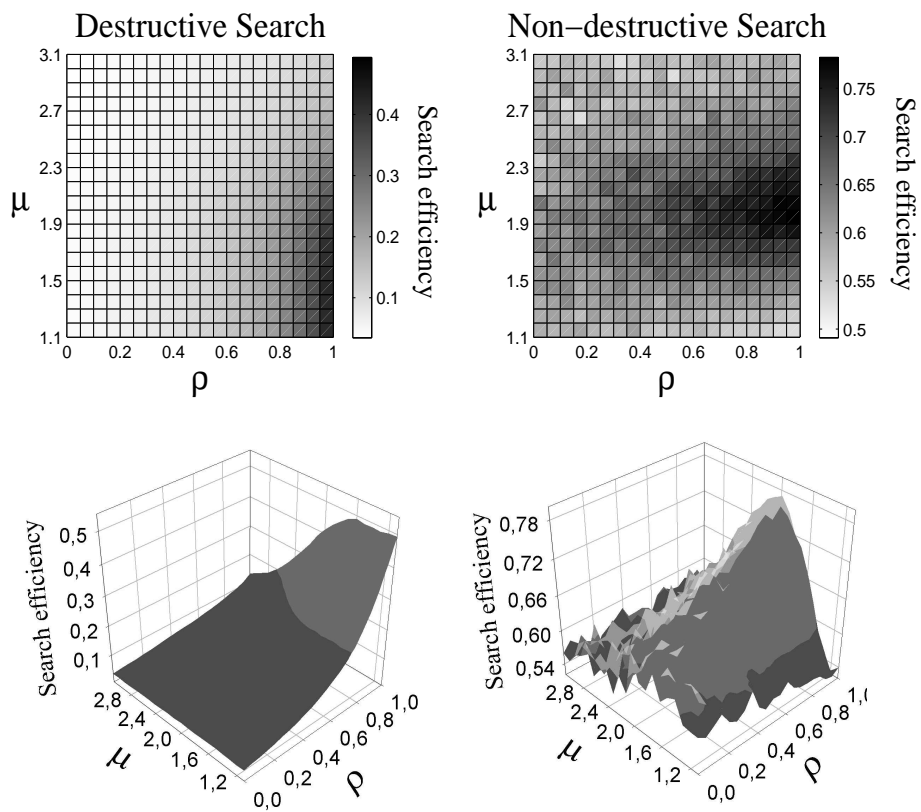


Figure 6.4: Search efficiency (measured as $\lambda\eta$) of the Lévy-modulated correlated random walk, plotted as a function of the shape parameter ρ and the Lévy exponent μ . The graphs assume a target density of $\lambda = 5000$. Results are shown for destructive and non-destructive encounter dynamics.

during flights. This explains why LWs appear robust in their efficiency even with sinuous flights due to the embedded CRWs. However, persistence within flights cannot fall too low, (e.g., a proper range $0.8 < \rho < 1$), otherwise the pattern of move lengths will lose fractality (i.e., scale invariance) due to the highly sinusoidal and looping paths, and so no pure LWs will arise at the necessary scales. Note that for $\rho < 1$ a natural upper cutoff appears for the scale invariance, due to the correlation length of the embedded CRW, and thus super-diffusive behavior does not occur in LMCRWs.

6.5 Discussion

Most ecological interactions must necessarily begin with a physical encounter (i.e., *sensu strictu*) which usually takes place after an active or passive searching process. By a search we mean the process of looking for the presence of real or suspected objects of interest (i.e., food, mate, shelter, etc.) which we name “targets”. Random search strategies can only exist when there is some degree of uncertainty in the behavior of targets. When there is no search uncertainty, because both spatial and temporal behavior of targets are known (Garber, 1988), or because displacements are dictated by strong external cues (Hauser et al., 1975), the resulting animal movement cannot be considered a search. Those situations where the overall animal movement is mainly driven by strong internal navigation mechanisms (i.e., migrations) or environmental constraints (i.e., strong physical barriers) should also not be considered a search.

In any interactive process between individuals, the search is only a component among others. In foraging strategies we also may consider the handling times, pursuit costs, predation risks, discount decisions, prey selection, etc. These components can be subjected to optimization by natural selection, the search component being more or less relevant depending on the cognitive capacities of organisms and the predictability of its environment. The optimization of a search strategy involves the selection of a specific set of “rules of search” that enhances the probability of finding unknown located items.

6.5.1 Systematic and random search strategies

According to the characteristics of the “rules of search” we can classify the *continuum* of search strategies in two main types: systematic and random searches. In systematic searches, the rules to optimally cover a

given area are based on deterministic algorithms (i.e., fixed and organized plans), while in random searches these rules rely on stochastic processes (i.e., the sampling of probability distributions). Systematic search strategies only work when some *a priori* relevant (although partial) information about target characteristics or locations at “landscape-level” is available. The Archimedean spirals represent one of the most common systematic searching rules in homing behaviors (Bell, 1991; Turchin, 1998). As available information regarding positional, kinetic, or behavioral characteristics of targets decreases, systematic searches become less effective. In these situations, animals must attempt to move in such a way so as to optimize their chances of locating resources by increasing “the chances of covering certain regions”, and thus, different optimal solutions arise by merely embracing different random strategies (Viswanathan et al., 1999; Bartumeus et al., 2002; Raposo et al., 2003; Santos et al., 2004). An interesting example that illustrates a switch between the two types of search is provided by the homing behavior of a desert isopod (Hoffmann, 1983a,b). If an isopod misses the entrance of its burrow by a few millimeters, it must search for it. If the excursion has covered only a short distance, it searches following an Archimedean spiral pattern. If the burrow is not found during this initial phase, the animal extends its range, and moves in broad loops and meanders, returning repeatedly to the starting point of the search (Hoffmann, 1983a). Therefore, when pure systematic search fails, the isopod uses a mixture of systematic (i.e., returns to the starting point) and random (i.e., meandering) search.

The opposite case, the shift from random search strategies to systematic searches should reflect an increase in the predictability of the spatiotemporal behavior of targets. Foraging scenarios involving non-destructive searches may enhance the incorporation of systematic rules in relation to the spatial and temporal pattern of rewards (learned after repeated visits to the targets). This is the case of trapline foraging in bumble bees (Thomson, 1996; Thomson et al., 1997; Williams & Thomson, 1998). Hermit hummingbirds traplining also includes systematic “rules of thumb” to directly interfere with the search success of competitors (Gill, 1988). In this case, uncertainty arises in relation to how the others behave, and search rules relying on stochastic processes may become an option (particularly for those individuals repeatedly “failing” in their interactions). Therefore, in any given environment there might be a range of search strategies that can be successful, and individuals may differ in the search strategy used. As is recognized by authors, the extension to what learned systematic search mechanisms work in more complex situations remains uncertain (Gill, 1988; Williams & Thomson, 1998).

So far, animal search rules relying on stochastic processes are not considered in behavioral evolution because it is assumed that sensorial or cognitive improvements override the need of random search in nature. However, it should be considered that: (i) in some search processes a high degree of uncertainty is unavoidable, and (ii) in such scenarios, the success of the search can be improved by optimizing random search strategies.

6.5.2 Lévy walks and Correlated random walks

The key assumptions of CRWs involve the presence of directional persistence at certain scales. However, random walk models with short-ranged correlations, such as CRWs, converge to a Brownian motion (i.e., normal diffusive process) at certain time scales, not very long (Fig. 6.2b). Therefore, at large enough spatiotemporal scales when persistence breaks down, the macroscopic statistical properties of CRWs become the same as in uncorrelated random walks. This fact, which is part of the standard random walk theory, has been used to justify the usage of uncorrelated random walks and normal diffusion models in ecology (Okubo, 1980; Berg, 1983a). However, our results show that their properties do not allow the best optimal random searches if large enough spatiotemporal scales are of relevance. This might be the reason why other biological considerations such as dispersal risks or energetic costs are needed in order to obtain optimal solutions when these models are used as random search strategies (Cain, 1985; Zollner & Lima, 1999b). Indeed, these studies concluded that without biological constraints any random search strategy should be equally efficient. Our results show that this is not the case.

The key assumptions of LWs involve *super-diffusive* and *scale-invariant* phenomena and ensure: (1) departures from normal diffusion at all scales (Fig. 6.2b), and (2) the possibility of optimizing encounter rates just by pure statistical physics considerations in a wide range of different searching scenarios (Fig. 6.3). Commonly, departures from normal diffusion have been attributed to: (i) “large-scale oriented” movements of individuals (e.g., seasonal migration, landscape-cues, cognitive-maps, etc.), or (ii) physical barriers or corridors in the landscape that alter an organism otherwise random movement (Johnson et al., 1992). However, to exploit the *statistical advantages* provided by super-diffusion and scale-invariance is not necessary to assume cognitive mapping or high spatial memory capacities of organisms (as some recent models suggest (Gautestad & Mysterud, 2005)). Instead, simple “rules of thumb” in accordance with stochastic laws may be enough. Consistently, scale-invariant animal movement is a widespread phenomenon in nature, observed from microorganisms to large

vertebrates. Thus far, Lévy walk patterns have been observed in soil amoebas (Levandowsky et al., 1997), planktonic organisms (Bartumeus et al., 2003), bumble bees (Heinrich, 1979), seabirds (Viswanathan et al., 1996), large terrestrial herbivores (Marell et al., 2002), social cannids (Atkinson et al., 2002), arboreal primates (Ramos-Fernández et al., 2004), and Arctic seals (Austin et al., 2004).

6.5.3 Lévy walks as adaptive random search strategies

We can inquire whether situations where random strategies are the optimal solutions to a search problem occur with sufficient frequency (at least to significantly modify the fitness of the populations). And, if so, whether there are specific biological mechanisms on which natural selection could impinge to develop specific behavioral traits. Biological mechanisms optimizing the “chances of finding” unknown located items should not necessarily be the same as those allowing for the “detection” of such items. Probably, the selective pressures and the triggering stimuli are different in each case, and the combination of both mechanisms can provide a huge behavioral plasticity to adapt searches to widely different ecological scenarios.

Based on the standard theory of random walks (Okubo, 1980; Berg, 1983a), it seems reasonable to think that selective pressure on “local scanning mechanisms” may not influence the statistical macroscopic properties of the walk, although it can provide short-range correlations with the statistical properties of CRWs. In contrast, selective pressure on “episodic reorientation mechanisms” could modify these macroscopic properties, and therefore change the chances of finding unknown located items. Our quantitative results comparing LW and CRW searching efficiencies show that the optimization of random searches mainly depends on the optimal temporal execution of reorientation events (Fig. 6.3). Even when directional persistence within displacements is not really high, the temporal execution of reorientation events is the key factor controlling the main properties of the random walk (Fig. 6.4). This result supports previous studies demonstrating the robustness of LWs against short-scale “memory effects” (da Luz et al., 2001; Raposo et al., 2003). Therefore, random search strategies are not incompatible with short-scaled (in time or space) “memory effects” (i.e., local scanning mechanisms, systematic “rules of thumb”, etc).

Overall, we suggest that scale-free punctuations in animal movement (i.e stops, strong reorientations, behavioral distinctive interruptions during the walk, etc.) could be the basis for a stochastic organization of the search at landscape level. Some preliminary empirical results point

towards this hypothesis (Bartumeus et al., 2003). The heterotrophic dinoflagellate *Oxyrrhis marina* switches from an exponential to an inverse square power-law distribution of flight times (that is, from diffusive to super-diffusive behavior) when its prey *Rhodomonas sp.* decreases in abundance. The specific biological mechanism involved in this searching behavioral change are transient arrests of the longitudinal flagellum beat, which are observable by simple visual inspection of the animal's movement. Thus, continuous helical motion is interrupted by sudden changes in direction (i.e., reorientation leaps) that govern the long-term searching walk of this planktonic predator. Although Lévy walk patterns have been identified for a wide variety of organisms (Viswanathan et al., 1996; Levandowsky et al., 1997; Atkinson et al., 2002; Marell et al., 2002; Austin et al., 2004; Ramos-Fernández et al., 2004), the case study of *Oxyrrhis marina* is so far the only example where the biological mechanism generating a Lévy-type walk has been elucidated. The biological mechanisms generating Lévy walk patterns in other species remain to be investigated. In this sense, two questions should be answered first: Are these patterns caused by a random search strategy or have they emerged from complex behavioral processes, external drivers, etc.? Can we identify reorientation mechanisms within animal behavioral traits? We expect that further investigations about when and how organisms actively discretize their movements (O'Brien et al., 1990; Kramer & McLaughlin, 2001) will facilitate the finding of adaptive mechanisms capable of optimizing random search statistics.

Acknowledgments

F.B. thanks D. Alonso and P. Fernández for contributing in the first stages of analytical and numerical approaches to Lévy walk simulations. F.B. also thanks R.V. Solé and the Complex System Lab group for inspiring talks on Lévy walks and random searches. G.M.V. and M.G.E. da L. thank E. Raposo for fruitful discussions. Also CNPq and FAPCAL (G.M.V.), and CNPq, CT-Infro, CT-Energ, Capes, and Fundação Araucária (M.G.E. da L.) are acknowledged for research grants.

6.6 Appendix

6.6.1 Correlated random walks

Correlated random walk (CRW) models are constructed on the basis of an exponentially decaying distribution of move lengths with a non-uniform angular distribution of turning angles. The latter distribution controls the directional persistence, i.e., the degree of correlation, in the random walk. The circular Gaussian distribution and the wrapped Cauchy distribution (WCD) are typically used as probability distributions for the turning angles (Cain, 1985; Zollner & Lima, 1999b; Byers, 2001). By varying the shape of the non-uniform turning angle distribution one can modify the degree of correlation or directional persistence of a given path.

In our simulations for CRWs, for each new step of movement we select the turning angles (i.e., deviations from the previous direction) from a WCD (Batschelet, 1981; Haefner & Crist, 1994). We sample the WCD distribution by using the inversion method, i.e., we generate turning angle deviations from the WCD by inserting a uniform random variable, $0 \leq u \leq 1$, into the inverse of the cumulative distribution function. So, the angle deviation θ from a preferred direction ϕ is obtained from

$$\theta = \phi + 2 \arctan \left[\left(\frac{1-\rho}{1+\rho} \right) \tan \left[\pi \left(u - \frac{1}{2} \right) \right] \right]. \quad (6.1)$$

In the calculations we set $\phi = 0$, so the WCD accounts for the tendency, observed in many organisms, to go straight forward. ρ is the shape parameter of the WCD, which controls sinuosity, and to that extent, diffusiveness. We can change the relative straightness of the CRW by varying the shape parameter ρ (Fig. 6.1a). For $\rho = 0$ we obtain a uniform distribution with no correlation between successive steps, thus Brownian motion emerges. For $\rho = 1$ we get a delta distribution at 0° leading to straight-line searches (Fig. 6.1a,b).

The successive move lengths (ℓ) of the CRWs are randomly drawn from a Gaussian distribution centered at the minimum move length $\ell_0 = 1$ and with fixed standard deviation $\sigma = 1$. The visual aspect of CRWs can be checked in (Fig. 6.1b).

6.6.2 Lévy walks

Lévy walk (LW) models involve a uniform distribution for the turning angles, but a power-law distribution for the move lengths (i.e., the so-called flights). More precisely, LW models exploit a broad class of move or flight

length (ℓ) distributions named Lévy-stable distributions (Mandelbrot, 1977; Shlesinger et al., 1995). These distributions have relevant statistical properties related to the Generalized Central Limit Theorem. Consider distributions that follow the power law $P(\ell) = \ell^{-\mu}$. Sums of such variables converge to the Lévy stable distribution, with Lévy stable index $\alpha_L = \mu - 1$. If the power law exponent μ lies in the interval $2 \leq \mu < 3$, then the Lévy stable distribution of the sums of such variables also has a power-law form. For $\mu > 3$ the form of the Lévy stable distribution of the sums converges to a Gaussian distribution due to the Central Limit Theorem. Thus we recover Brownian motion for $\mu \geq 3$. The case of $\mu \leq 1$ does not correspond to normalizable distributions.

In practice, we generate Lévy flights by sampling a power-law distribution (representing the tail of the Lévy-stable distributions) in the following way (inversion method, see CRWs)

$$\ell = \ell_0 u^{(1-\mu)^{-1}}. \quad (6.2)$$

Where u is a uniformly distributed random variable ($u \in (0, 1)$), ℓ_0 is the minimum flight length (in our LW simulations $\ell_0 = 0.1$) and μ the power-law exponent. To obtain a LW model, once a move length (i.e., a flight) and a direction become sampled from the respective distributions, the searcher then “walks” in a straight-line motion until reaching the specified move length. In LWs, directional persistence intrinsically occurs because of the power-law distribution of move lengths (Fig. 6.1c). This feature explains the existence of ultra-long straight travels in LWs, which are rarely or never observed in CRWs. As μ diminishes the probability of long travels increases, thus the directional persistence in the movement also increases. LW models thus comprise a rich variety of paths ranging from Brownian motion ($\mu \geq 3$) to straight-line paths ($\mu \rightarrow 1$) (Fig. 6.1d).

6.6.3 Lévy-modulated correlated random walks

If we relax the condition of straight-line move lengths of LW models by introducing a CRW behavior during a LW move length period, we then obtain a new model. We have named this new random walk model the Lévy-modulated correlated random walk (LMCRW). In the LMCRW model, the flights consist of a series of steps correlated through a series of turning angles randomly drawn from a WCD. The length of the steps within a flight are randomly drawn from a Gaussian distribution with $\ell_0 = 1$ and $\sigma = 1$ until reaching the specified Lévy flight length. Thus, the LMCRW model generates a random walk with (i) a WCD for the turning angles within a flight, (ii) a Gaussian distribution of move steps within a flight, (iii) a uniform

distribution for the turning angles between flights, and (iv) a power-law distribution of flight lengths. As in the LW model, the directional persistence of LMCRW is also introduced through a power-law distribution of move lengths (i.e., flights) but we can also modulate or control the degree of directional persistence during flight lengths through a WCD of turning angles. Indeed, flight lengths are not necessarily related to a fixed walking distance because of the existence of turning angles deviations within flights.

6.6.4 Mean square displacement simulations

In two dimensional systems, the mean squared displacement from a starting reference point (x_0, y_0) of a population of N random walkers at a given time t is computed as,

$$\langle R(t)^2 \rangle = \frac{1}{N} \sum_{i=1}^N [(x_i(t) - x_0)^2 + (y_i(t) - y_0)^2]. \quad (6.3)$$

where $x_i(t)$ and $y_i(t)$ are the cartesian positions at time t of individual i . The scaling behavior of msd with time ($\langle R(t)^2 \rangle \sim t^\alpha$) characterizes the spreading rate of diffusive processes. A value $\alpha = 1$ indicates normal diffusion and $\alpha \neq 1$ indicates anomalous diffusion. Superdiffusion leads to $\alpha > 1$.

The mean squared displacement (msd) is a traditional metric of random walk theory (Berg, 1983a; Shlesinger et al., 1995). In the context of statistical physics and the study of random walk diffusive properties, the msd involves an ‘‘averaging’’ process over an ensemble of random walking particles. A measure of α can also be obtained from a single random walk, if the population average is replaced by a time average, as is done in Hurst analysis and similar methods. We have computed the msd for LWs and CRWs by ‘‘averaging’’ over ensembles of Lévy and correlated random walkers respectively. In Kareiva & Shigesada (1983) the msd for correlated random walkers is calculated analytically and named *expected net square displacement*. Under specific sets of parameters, the msd averaged over an ensemble of correlated random walkers and the *expected net square displacement* should coincide.

6.6.5 Search efficiency simulations

We assume that the search is performed in an homogeneous bidimensional space, with target sites distributed randomly. The searcher moves with constant speed and with random directions and move lengths chosen from their respective distributions. During a walking step, if a target site lies

within a direct detection distance or radius r_d , then we register an encounter. That walking step is then truncated and the searcher starts a new displacement by selecting a new direction and a new move length from the respective probability distributions. As both the searchers and the target sites can be represented as circles, we should consider both the detection radius of the searcher r_d and the radius of the target sites r_t . However, this is equivalent to consider a detection radius $R = r_d + r_t$ and the target sites as points in the space $r_t = 0$.

The whole search process is scaled on the basis of the mean free path parameter λ . The size of the system (L), the number of target sites (N_t) and the detection distance or radius (r_d) set the mean free path (λ). In a random searching process, we can express λ as the average distance between two target sites. This distance is inversely related to the target sites number N_t and the radius R , and directly related to the search area L^2 , where L is the one-dimensional size of the system. For two dimensional systems we have,

$$\lambda \approx \frac{L^2}{2RN_t}. \quad (6.4)$$

Without loss of generality we fixed the minimum step length $l_0 = r_d = 0.5$, $R = 1$ and $N_t = 25$. Then, we choose $\lambda = 100, 1000$, and 5000 to represent a decreasing gradient in the density of target sites, and we finally computed L from Eq. 6.4. Note that several combinations of the parameters r_d , N_t , and L leading to the same λ will give the same results. In this sense, search scenarios are described by a unique parameter λ which is the key scaling parameter with space dimensional units. Since our interest lies in *long-term* search statistics we perform walks of 10^7 steps and compute the search efficiency function η as the ratio of the number of target sites visited to the total distance traversed by the searcher.

Our focus relates to the search efficiency of a free-ranging behavior within a wide range of scales. Thus, in these simulations, we represent an effectively infinite landscape by means of periodic space boundaries (i.e., organisms leaving the landscape on one side emerge from the opposite side). Although landscapes with no edges do not exist, the statistics obtained with this procedure has greater precision than with reflecting or absorbing boundary conditions. In these simulations, reactive behaviors occur only due to encounter processes but never due to other aspects, such as landscape barriers or fragmentation, not considered here.

The software has been developed on C++ programming language and Linux environment. Simulations involve high-computational costs and optimization procedures have been used to compute search efficiency averages. In the simulations several searchers are moving at the same time to

improve the statistics and optimize computational costs. The searchers do not interfere between them, and the overall dynamics is also not altered.